Chemical Engineering Journal 164 (2010) 132–138

Contents lists available at ScienceDirect

Chemical Engineering Journal

journal homepage: www.elsevier.com/locate/cej

Kinetics of oxidation of total sulfite in the ammonia-based wet flue gas desulfurization process

Yong Jia, Qin Zhong*, Xueyou Fan, Xinrong Wang

School of Chemical Engineering, Nanjing University of Science and Technology, Nanjing 210094, China

ARTICLE INFO

Article history:
Received 4 March 2010
Received in revised form 30 July 2010
Accepted 17 August 2010

Keywords:
Kinetics
Total sulfite
Oxidation
Bubbling reactor
Mass transfer
Mathematical model

ABSTRACT

Using bubbling apparatus, the kinetics of oxidation of total sulfite in ammonia-based wet flue gas desulfurization (FGD) process was investigated by varying concentrations of SO_3^{2-} and SO_4^{2-}, pH, temperatures and air flow. The concentration range of sulfite is 0.0044–0.026 gmol L^{-1} and that of sulfate is 0.5–2 gmol L^{-1}. Experiments were conducted at pH level of 4.5–6.5 and air flow ranging from 50 to 200 L h^{-1}. In the temperature range of 303.15–333.15 K, the reaction was found to be −0.5 order with respect to sulfite. The experimental findings also showed that the bisulfite could be oxidized easier than sulfite. Thus, keeping the pH level of the solution low is conducive to the oxidation of total sulfite. The apparent activation energy for the overall oxidation was calculated to be 28.0 kJ mol^{-1}. A kinetic model has been derived according to the experimental results. The developed kinetic model, including the operating parameters SO_3^{2-} concentration, SO_4^{2-} concentration, pH, temperature and air flow, can be applied to simulate the oxidation of total sulfite. This model would be useful for the design of the ammonia-based wet FGD system.

Crown Copyright © 2010 Published by Elsevier B.V. All rights reserved.

1. Introduction

Among the various flue gas desulfurization processes, the wet-type techniques using ammonia as an absorbent lead to efficient removal of SO_2. Ammonium sulfite thus formed can be oxidized to ammonium sulfate which is used as a fertilizer [1–3]. The ammonia-based wet FGD process is attractive as it results in the production of valuable ammonium sulfate without generating any other polluting by-products, according to the following oxidation reaction [4]:

$$(NH_4)_2SO_3 + 1/2O_2 \rightarrow (NH_4)_2SO_4 \quad (1)$$

$$NH_4HSO_3 + 1/2O_2 \rightarrow NH_4HSO_4 \quad (2)$$

In the chemical engineering literature the problem of oxidation of aqueous ammonium sulfite has been studied by a number of investigators. Mishra and Srivastava conducted a study of the kinetics of the homogeneous oxidation of ammonium sulfite using the rapid mixing method of Hatridge and Roughton. The reaction rate was found to be 0 order with respect to oxygen, 2/3 order with respect to sulfite and 0.5 order with respect to cobalt [5]. Neelakantan and Gehlawat studied the kinetics of absorption of oxygen in aqueous solutions of ammonium sulfite in stirred cells. In the range of the ammonium sulfite concentration of 0.045–0.45 mol L^{-1} the reaction was found to be 2 order with respect to sulfite and 1 order with respect to oxygen [6]. Ahmad et al. found the reaction to be 0 order with respect to sulfite above a critical sulfite concentration, 2 order below a critical sulfite concentration, and 1 order in oxygen [7]. Gŭrkan et al. investigated the kinetics of the heterogeneous oxidation of ammonium sulfite with oxygen transferring from the gas phase and proposed that the reaction mechanism and consequently the order of the intrinsic rate of reaction were dependent on the oxygen to sulfite ratio [8]. Recently Zhou et al. found the reaction to be 1 order with respect to oxygen, 0.2 order with respect to sulfite above a critical sulfite concentration and −1.0 order below a critical sulfite concentration [9].

Although the oxidation of ammonium sulfite has been extensively studied for many years, kinetics analysis has been slow in developing. It should be noted that most of these previous investigations dealt with oxygen absorption into basic sulfite solutions and did not take the oxidation of ammonium bisulfite into consideration [5–11], under conditions significantly different from those encountered in ammonia-based wet FGD plants. In previous investigations, the pH was significantly different from that in the plants, Ahamd controlled pH level at range of 7.6–8.5, Gŭrkan controlled pH at range of 7.0–8.0 and Zhou controlled pH at range of 5.0–8.0 [8–10]. In the literature, sulfuric acid (or hydrochloric acid) and ammonia were used to adjust the pH. Changes in the pH resulted in changes in the ionic strength, which influenced the oxidation rate. This has not been taken into account in the previous investi-

* Corresponding author. Tel.: +86 025 84315517; fax: +86 025 84315517.
E-mail addresses: jiayong2000@163.com (Y. Jia), Zq304@mail.njust.edu.cn (Q. Zhong).

1385-8947/$ – see front matter. Crown Copyright © 2010 Published by Elsevier B.V. All rights reserved.
doi:10.1016/j.cej.2010.08.041

Nomenclature

a	specific gas–liquid interfacial area ($m^2\ m^{-3}$)
$C_{SO_4^{2-}}$	concentration of sulfate ($mol\ L^{-1}$)
$C_{SO_3^{2-}}$	concentration of sulfite ($mol\ L^{-1}$)
$C^*_{O_2}$	interfacial concentration of oxygen ($mol\ L^{-1}$)
C_{O_2}	concentration of oxygen in the solution ($mol\ L^{-1}$)
D_{O_2}	diffusion coefficient of oxygen ($m^2\ s^{-1}$)
D_R	diameter of bubbling reactor (m)
d_{VS}	volume–surface mean bubble diameter (m)
g	gravitational constant ($m\ s^{-2}$)
H	solubility coefficient of SO_2 in solution ($mol\ m^{-3}\ Pa^{-1}$)
H^0	solubility coefficient of SO_2 in water ($mol\ m^{-3}\ Pa^{-1}$)
h	proportionality constant ($m^3\ kion^{-1}$)
I	ionic strength ($kion\ m^{-3}$)
$Ka1$	equilibrium constant, $\log Ka1 = 853/T - 4.74$
$Ka2$	equilibrium constant, $\log Ka2 = 621.9/T - 9.278$
$Ka3$	equilibrium constant
$Ka4$	equilibrium constant
Kw	equilibrium constant, $\log Kw = 4470.99/T + 6.0875 - 0.01706$
k	the reaction constant
k_0	frequency factor
k_G	gas-phase mass transfer coefficient ($mol\ m^{-2}\ s^{-1}\ Pa^{-1}$)
k_L	liquid-phase mass transfer coefficient ($m\ s^{-1}$)
$p^*_{O_2}$	partial pressure of oxygen on the gas–liquid interface (Pa)
R	gas constant ($8.31\ J\ mol^{-1}\ K^{-1}$)
$r_{(IV)}$	the oxidation rate of total sulfite ($mol\ L^{-1}\ min^{-1}$)
T	temperature (K)
t	time (min)
u_{OG}	superficial gas velocity ($m\ s^{-1}$)

Greek symbols

δ_0	distribution coefficient of SO_2(aq)
δ_1	distribution coefficient of HSO_3^-
δ_2	distribution coefficient of SO_3^{2-}
ε_G	gas holdup (%)
μ_L	viscosity of solution (Pa s)
ρ_L	density of solution ($kg\ m^{-3}$)
σ_L	surface tension of solution ($N\ m^{-1}$)

Subscript

i	the species of electrolyte in the solution

gations. Thus, the detailed information on the kinetics of oxidation of sulfite in the literature is not available for ammonia-based wet FGD process. An independent study is needed. The present work was undertaken to make a systematic study of the kinetics of oxidation of total sulfite (SO_2(aq), $(NH_4)_2SO_3$ and NH_4HSO_3), under operating conditions relevant to ammonia-based wet FGD plants.

2. Experimental

The oxidation of total sulfite was carried out in a bubbling reactor. Fig. 1 shows the schematic diagram for experimental setup. The bubbling reactor used is a glass cylindrical vessel, 10.8 cm in internal diameter and 19 cm in height. Before performing the experiment, 500 ml of distilled water was added into the bubbling reactor which was installed in a constant-temperature bath. The pH was then adjusted by passing SO_2 gas through the solution after a

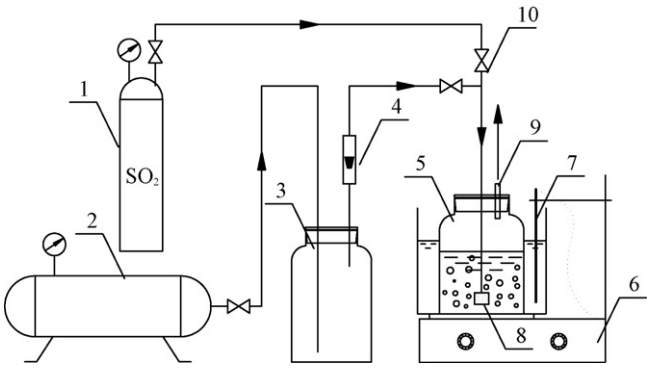

Fig. 1. Experimental apparatus. (1) SO_2 tank; (2) air compressor; (3) buffer tank; (4) air flow meter; (5) bubbling reactor; (6) constant-temperature bath; (7) thermocouple; (8) aeration header; (9) sampling port; (10) valve.

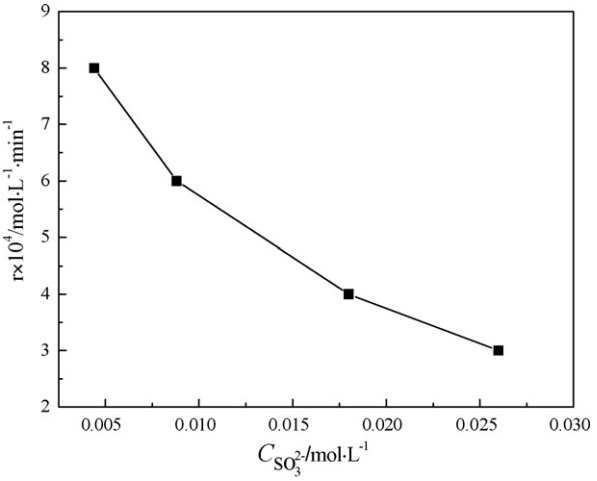

Fig. 2. Effect of sulfite concentration on the oxidation rate. $Q = 100\ L\ h^{-1}$; $C_{SO_4^{2-}} = 1\ mol\ L^{-1}$; pH = 5.5; $T = 313.15$ K.

certain amount of ammonium sulfite and ammonium sulfate were added into the bubbling reactor. Finally, the time was noted and the air was injected into the solution in a steady manner.

Experiments were conducted at pH level of 4.5–6.5, under conditions where the concentration of HSO_3^- was much larger than

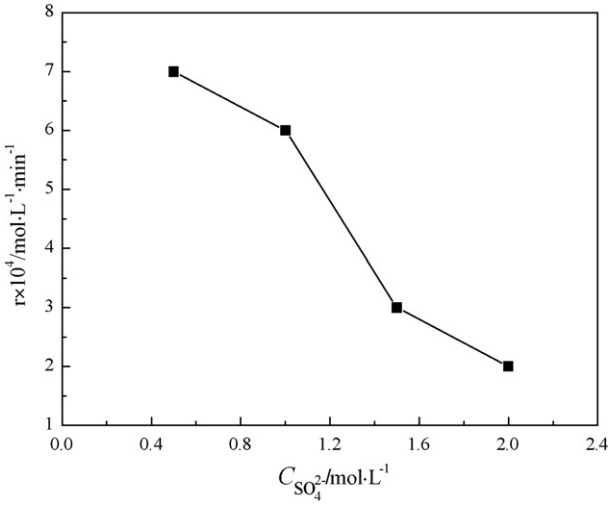

Fig. 3. Effect of sulfate concentration on the oxidation rate. $Q = 100\ L\ h^{-1}$; $C_{SO_3^{2-}} = 0.01\ mol\ L^{-1}$; pH = 5.5; $T = 313.15$ K.

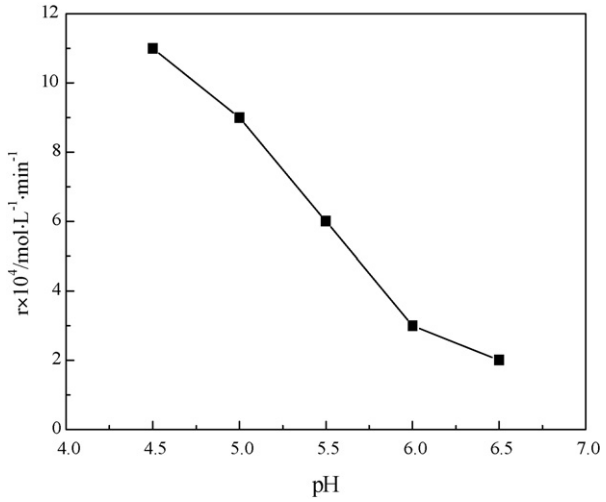

Fig. 4. Effect of pH on the oxidation rate. $Q = 100\,L\,h^{-1}$; $C_{SO_3^{2-}} = 0.01\,mol\,L^{-1}$; $C_{SO_4^{2-}} = 1\,mol\,L^{-1}$; $T = 313.15\,K$.

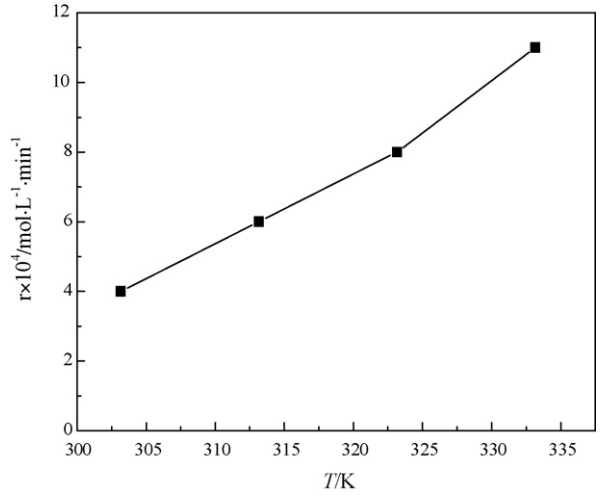

Fig. 5. Effect of temperature on the oxidation rate. $Q = 100\,L\,h^{-1}$; $C_{SO_3^{2-}} = 0.01\,mol\,L^{-1}$; $C_{SO_4^{2-}} = 1\,mol\,L^{-1}$; pH = 5.5.

that of SO_3^{2-}. Thus, the experiments were conducted at different concentration of SO_3^{2-} between 0.0044 and 0.026 mol L^{-1}.

According to the chemical equilibrium, the concentration of SO_2(aq) in the solution can be ignored at this pH range. The total sulfite concentration ($C_{S(IV)} = C_{SO_3^{2-}} + C_{HSO_3^-}$) was determined by means of iodometric titrations at intervals of 30 min. Similarly, the sulfate concentration was measured by means of ion chromatography. Although the oxidation rate of SO_3^{2-} and that of HSO_3^- are difficult to measure separately, it should be noted that the oxidation rate of total sulfite is equal to the variation rate of sulfate concentration ($r_{(IV)} = dC_{SO_4^{2-}}/dt$) during the experiment. The oxidation rate of total sulfite can be evaluated by the method of initial rates [12].

3. Theoretical

The rate of oxidation reaction can be written as the product of a reaction rate constant k and a function of the concentrations of the various species involved in the reaction, i.e. [12],

$$r_{(IV)} = [k(T)][fn(C_A, C_B, \ldots)] \quad (3)$$

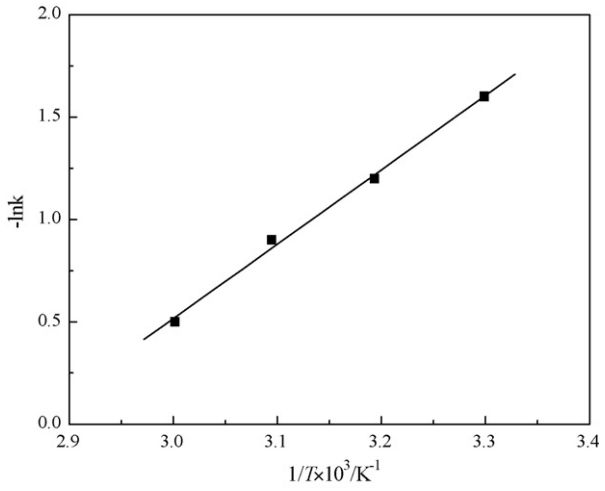

Fig. 6. Variation of reaction constant with temperature.

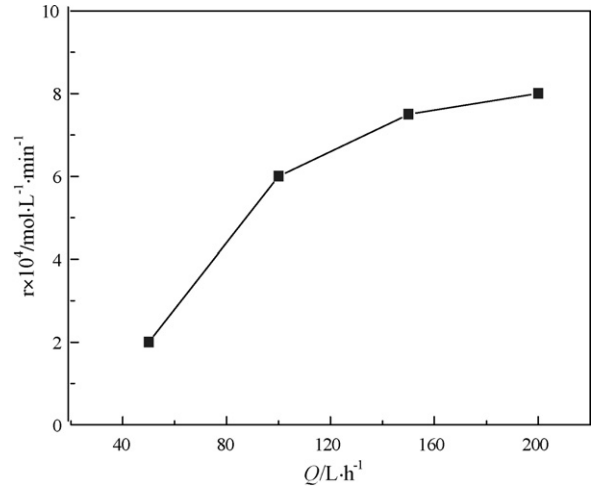

Fig. 7. Effect of air flow on the oxidation rate. $C_{SO_3^{2-}} = 0.01\,mol\,L^{-1}$; $C_{SO_4^{2-}} = 1\,mol\,L^{-1}$; $T = 313.15\,K$; pH = 5.5.

The reaction rate constant could be correlated by the Arrhenius formula:

$$k(T) = k_0\ e^{-E/RT} \quad (4)$$

The activation energy E and frequency factor k_0 are determined experimentally by carrying out the reaction at several different temperatures. After taking the nature logarithm of Eq. (4):

$$\ln k = \ln k_0 - \frac{E}{R}\left(\frac{1}{T}\right) \quad (5)$$

It can be seen that a plot of $\ln k$ versus $1/T$ should be a straight line whose slope is proportional to the activation energy. The dependence of the reaction rate $r_{(IV)}$ on the concentrations of the species present, $fn(C_j)$, is determined by experiments.

4. Results and discussion

4.1. Effect of SO_3^{2-} concentration

A number of experiments were performed at various SO_3^{2-} concentrations to demonstrate its effect on the oxidation rate of total sulfite, keeping pH at 5.5. In the solution, there are nine different species, i.e. HSO_3^-, SO_3^{2-}, HSO_4^-, SO_4^{2-}, OH^-, H^+, NH_4^+, $NH_3{\cdot}H_2O$ and SO_2(aq), among which the following chemical equilibriums

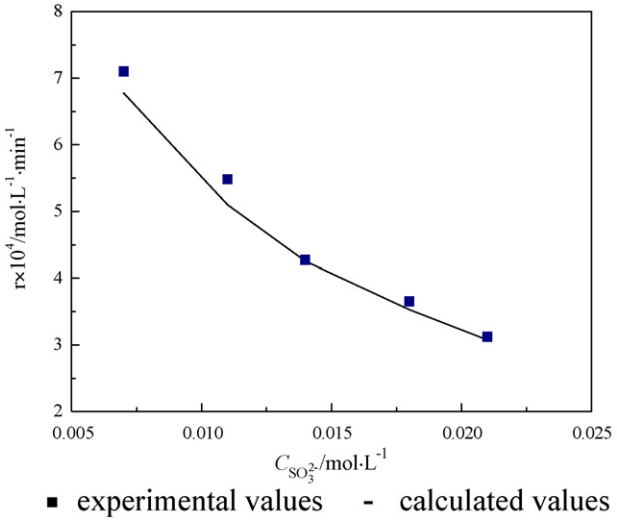

Fig. 8. Effect of sulfite concentration on the oxidation rate. $Q = 140\,L\,h^{-1}$; $C_{SO_4^{2-}} = 1.4\,mol\ L^{-1}$; pH = 5.4; $T = 313.15\,K$. (■) Experimental values; (□) calculated values.

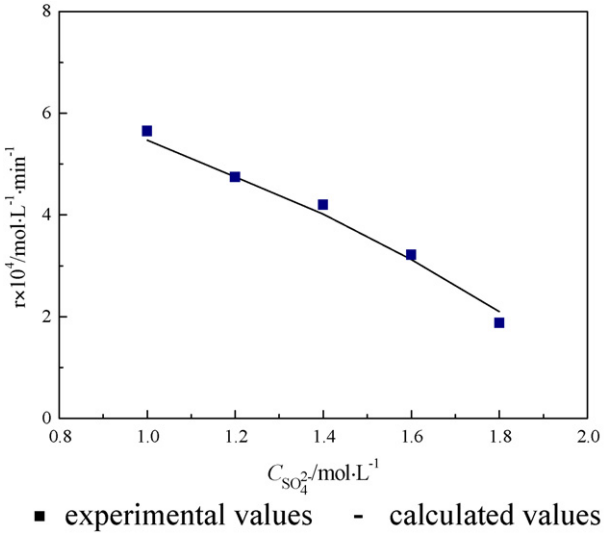

Fig. 9. Effect of sulfate concentration on the oxidation rate. $Q = 140\,L\,h^{-1}$; $C_{SO_3^{2-}} = 0.015\,mol\ L^{-1}$; pH = 5.4; $T = 313.15\,K$. (■) Experimental values; (□) calculated values.

take place [1,2,13]:

$$SO_2(aq) + H_2O(l) \overset{K_{a1}}{\rightleftarrows} H^+ + HSO_3^- \quad (6)$$

$$HSO_3^- \overset{K_{a2}}{\rightleftarrows} H^+ + SO_3^{2-} \quad (7)$$

$$NH_3 \cdot H_2O \overset{K_{a3}}{\rightleftarrows} NH_4^+ + OH^- \quad (8)$$

$$HSO_4^- \overset{K_{a4}}{\rightleftarrows} H^+ + SO_4^{2-} \quad (9)$$

$$H_2O \overset{K_w}{\rightleftarrows} H^+ + OH^- \quad (10)$$

The distribution coefficient of each species of total sulfite is as follows:

$$\delta_0 = \frac{[H^+]^2}{[H^+]^2 + K_{a1}[H^+] + K_{a1}K_{a2}} \quad (11)$$

$$\delta_1 = \frac{K_{a1}[H^+]}{[H^+]^2 + K_{a1}[H^+] + K_{a1}K_{a2}} \quad (12)$$

$$\delta_2 = \frac{K_{a1}K_{a2}}{[H^+]^2 + K_{a1}[H^+] + K_{a1}K_{a2}} \quad (13)$$

The ratio of SO_3^{2-} concentration to HSO_3^- concentration is a function of pH according to Eqs. (12) and (13). Therefore concentration of SO_3^{2-} and HSO_3^- can be evaluated by taking into account simultaneously the chemical equilibrium corresponding to reactions (6)–(10), as well as pH.

Fig. 2 shows the variation of the oxidation rate of total sulfite with SO_3^{2-} concentration. It is observed that the oxidation rate of total sulfite decreases as SO_3^{2-} concentration increases. The oxidation rate of total sulfite is found to be −0.5 order with respect to SO_3^{2-} and with a correlation coefficient of 0.99. Neelakantan reported the reaction to be 2 order with respect to sulfite. Gŭrkan found the reaction to be 2 order with respect to sulfite above a critical sulfite concentration, 0 order below a critical sulfite concentration. However, Zhou reported the reaction to be 0.2 order with respect to sulfite above a critical sulfite concentration, −1.0 order below a critical sulfite concentration. In these literature, the experimental conditions (e.g. sulfite concentration and pH) were different and the oxidation of bisulfite was not taken into consideration. Thus, these previous results are controversial.

4.2. Effect of SO_4^{2-} concentration

The relation of oxidation rate of total sulfite versus SO_4^{2-} concentration is shown in Fig. 3.

It is obvious that the oxidation rate is almost inversely proportional to the sulfate concentration. The similar tendency has also been reported by Zhou [9]. An examination of Fig. 3 reveals that the experimental data can be linearized as $r_{S(IV)} = 0.0001 \times (9 - 4C_{SO_4^{2-}})$ with a correlation coefficient of 0.99. Therefore, it can be deduced from this equation that if the solution includes too much sulfate, the oxidation rate of total sulfate will be inhibited to a considerably low value. Gŭrkan and Zhou also noticed that the total ionic strength of sulfate could influence the oxidation rate. The reason that sulfate ion hampers the oxidation may be due to the decrease of the solubility of oxygen in the solution [14,15].

4.3. Effect of pH

Typical experimental results indicating the dependence of pH on the oxidation rate of total sulfite are shown in Fig. 4. An examination of Fig. 4 shows that the oxidation rate of total sulfite decreases as pH increases. Zhou and Wang reported that the oxidation rate of sulfite decreases with the increase of pH [9,16]. At a pH level of 7–8, Gŭrkan et al. found that the oxidation rate of sulfite increases as pH increases [8]. Zhou adjusted the pH by adding sulfuric acid into the solution. Wang adjusted the pH by using hydrochloric acid and ammonia, while Gŭrkan used ammonia to adjust the pH. The ionic strength of sulfate and other ions could influence the reaction rate [8,9]. Thus, the existence of the acid radical and ammonium ions added into solution would affect the accuracy of the experimental results.

In the present work, pH was adjusted by passing SO_2 through the solution. Thus, the influence of the acid radical and ammonium ions on the oxidation rate can be eliminated. According to Eqs. (12) and (13), the concentration of SO_3^{2-} and HSO_3^- can be evaluated by taking into account the total sulfite and pH. By linear fitting the experimental data, the oxidation rate of total sulfite can be expressed as $r_{S(IV)} = \exp(-0.39pH - 1.14)$ with a correlation coefficient is 0.97. This expression is similar to that proposed by Gerbec et al. [17].

An examination of Fig. 4 also reveals that the bisulfite can be oxidized easier than sulfite. According to Eqs. (11)–(13), the ratio

of bisulfite concentration to sulfite concentration increases with the pH decrease. Therefore keeping the pH level of the solution low is conducive to the oxidation of total sulfite. However, the control of pH in the wet ammonia-based process should take corrosiveness as well as the absorption of SO_2 into account.

4.4. Effect of temperature

Temperature plays an important role in the oxidation of total sulfite. A number of experiments were performed at different temperature to demonstrate its effect on the oxidation rate. Experimental results are shown in Fig. 5. It is obvious that the oxidation rate of total sulfite increases as the temperature increases. The same tendency has been reported by Gŭrkan et al., Zhou et al., and Wang and Zhao [8,9,16].

A plot of the logarithm of reaction constant versus $1/T$ is shown in Fig. 6. An examination of Fig. 6 reveals that the reaction constant increases with a rise in temperature. That is why the oxidation rate of total sulfite increases as the temperature increases. According to Eq. (5), the apparent activation energy for the overall oxidation was calculated to be 28.0 kJ mol^{-1}, which is close to that proposed by Zhou et al. [9]. However this value is higher than the activation energy previously reported by Gŭrkan et al. [8]. The reason could be that the catalyst wasn't used in our work, while it was used in Gŭrkan's investigations.

4.5. Effect of air flow

The effect of air flow on the oxidation rate of total sulfite is shown in Fig. 7. An examination of Fig. 7 shows that the oxidation rate of total sulfite increased quickly with the air flow up to 150 L h^{-1}, above which it increased slowly. This tendency is similar to that reported by Wang and Zhao [16]. The reason may be that the gas–liquid contact area increased as the air flow increased while below 150 L h^{-1}. On the other hand, the stirring effect of air on the solution became more evident with a rise in air flow below 150 L h^{-1}. When the air flow was increased to 150 L h^{-1}, some air froth collided and agglomerated, resulting in a little change of gas–liquid contact area and the stirring effect on the solution [16].

4.6. Kinetic model

Investigators such as Neelakantan found that the oxidation reaction was 1 order with respect to oxygen [6–9]. Accordingly, the oxidation reaction is assumed to be 1 order with respect to oxygen in this work. Basing on the experimental results above, the following rate expression can be derived:

$$r_{(IV)} = k_0 \exp\left(\frac{-2.8\times10^4}{RT}\right) \times 10^{(-0.39\mathrm{pH}-1.14)} \cdot C_{SO_3^{2-}}^{-0.5} \cdot (-0.0004C_{SO_4^{2-}} + 0.0009) \cdot C_{O_2} \quad (14)$$

The oxidation process of total sulfite could be divided into two steps: oxygen transfer from gas phase to the solution; reaction between oxygen and total sulfite in the liquid phase. The mass transfer rate of oxygen is equal to the oxidation rate of total sulfite at steady-state conditions. So the following equation can be obtained according to the double-film theory [18]:

$$r_{(IV)} = k_L a(C_{O_2}^* - C_{O_2}) \quad (15)$$

Combining Eqs. (14) and (15), the concentration of dissolved oxygen can be expressed as:

$$C_{O_2} = \frac{k_L a C_{O_2}^*}{k_0 \exp(-2.8\times10^4/RT) \times 10^{(-0.39\mathrm{pH}-1.14)} \cdot C_{SO_3^{2-}}^{-0.5} \cdot (-0.0004C_{SO_4^{2-}} + 0.0009) + k_L a} \quad (16)$$

By combining Eqs. (14)–(16) to eliminate the concentration of dissolved oxygen, one obtains:

$$r_{(IV)} = \frac{C_{O_2}^*}{(1/k_L a) + (1/k_0 \exp(-2.8\times10^4/(RT))) \cdot (1/10^{(-0.39\mathrm{pH}-1.14)}) \cdot (1/C_{SO_3^{2-}}^{-0.5}) \cdot (10000/(-4C_{SO_4^{2-}} + 9))} \quad (17)$$

According to Henry's Law, the interfacial concentration of oxygen can be expressed in the following form [18–20]:

$$C_{O_2}^* = Hp_{O_2}^* \quad (18)$$

where

$$\log\left(\frac{H^0}{H}\right) = h_1 I_1 + h_2 I_2 + \cdots + h_i I_i + \cdots \quad (19)$$

In Eq. (19), I is the ionic strength and h is the proportionality constant. The proportionality constant is the sum of contributions referring to the species of positive and negative ions and to the species of gas as:

$$h_i = h^+ + h^- + h_G \quad (20)$$

The liquid-phase mass transfer coefficient k_L can be written as [21]:

$$k_L = 0.5\frac{D_{O_2}}{d_{VS}}\left(\frac{\mu_L}{D_{O_2}\rho_L}\right)^{0.5}\left(\frac{g d_{VS}^3 \rho_L^2}{\mu_L^2}\right)^{0.25}\left(\frac{g d_{VS}^2}{\sigma_L}\right)^{0.375} \quad (21)$$

where

$$d_{VS} = 26 D_R \left(\frac{g D_R^2}{\sigma_L}\right)^{-0.5}\left(\frac{g D_R^3 \rho_L^2}{\mu_L^2}\right)^{-0.12}\left(\frac{u_{OG}}{\sqrt{g D_R}}\right)^{-0.12} \quad (22)$$

The specific gas–liquid interfacial area a is related to the fractional gas holdup ε_G and the volume–surface mean bubble diameter d_{VS} by following equation [21]:

$$a = \frac{6\varepsilon_G}{d_{VS}} \quad (23)$$

The gas holdup in the bubbling reactor was defined by:

$$\frac{\varepsilon_G}{(1-\varepsilon_G)^4} = 0.25 \times \left(\frac{u_{OG}\mu_L}{\sigma_L}\right)\left(\frac{\rho_L \sigma_L^3}{g\mu_L^4}\right)^{7/24} \quad (24)$$

Combining Eqs. (17)–(23), the rate expression for the oxidation of total sulfite can be expressed as:

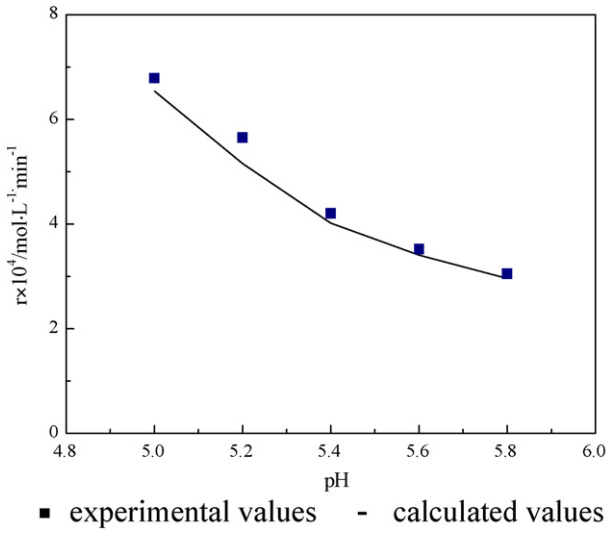

Fig. 10. Effect of pH on the oxidation rate. Q = 140 L h^{-1}; $C_{SO_3^{2-}}$ = 0.015 mol L^{-1}; $C_{SO_4^{2-}}$ = 1.4 mol L^{-1}; T = 313.15 K. (■) Experimental values; (□) calculated values.

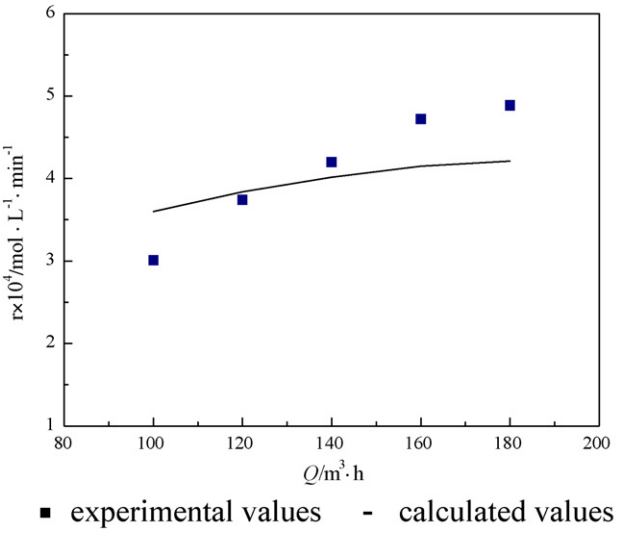

Fig. 12. Effect of air flow on the oxidation rate. $C_{SO_3^{2-}}$ = 0.015 mol L^{-1}; $C_{SO_4^{2-}}$ = 1.4 mol L^{-1}; T = 313.15 K; pH = 5.4. (■) Experimental values; (□) calculated values.

$$r_{(IV)} = \frac{Hp^*_{O_2}}{(1/k_L a) + (1/k_0 \exp(-2.8 \times 10^4/(RT)) \times 10^{-4}) \cdot (1/10^{(-0.39pH-1.14)}) \cdot (1/C^{-0.5}_{SO_3^{2-}}) \cdot (1/(-4C_{SO_4^{2-}} + 9))} \quad (25)$$

4.7. Simulation of the oxidation process

Using the kinetic model derived, the oxidation process of total sulfite was simulated at different operating conditions. The calculated (line) and the experimental (points) oxidation rate are compared in Figs. 8–12. In particular, the model parameters are presented in Tables 1 and 2.

As shown in Figs. 8–10, the calculated values for the operating conditions SO_3^{2-} concentration, SO_4^{2-} concentration and pH closely correspond to the experimental values.

Fig. 11 illustrates the influence of operating condition T for the oxidation rate. Obviously, both the calculated values and the experimental results increase as temperature increases. It is worth noting that the agreement is satisfactory with temperatures up to 323.15 K, above which the experimental results increase more rapidly than calculated values. The reasons may be that the decomposition of sulfite increases as the temperature increases, which cannot be simulated by using this model. In the ammonia-based wet FGD plants, the operating temperature of the spray scrubber is usually controlled at about 323.15 K. The relative error of the calculated oxidation rate is about 15.3% at a temperature of 323.15 K. Thus, this model is appropriately used to simulate the effect of temperature on the oxidation of total sulfite.

Fig. 12 illustrates the influence of operating condition air flow on the oxidation rate of total sulfite. It can be seen that the oxidation rate increases with air flow increase. The tendency of the calculated values is similar to that of the experimental values. However, the experimental values increase more rapidly than the calculated val-

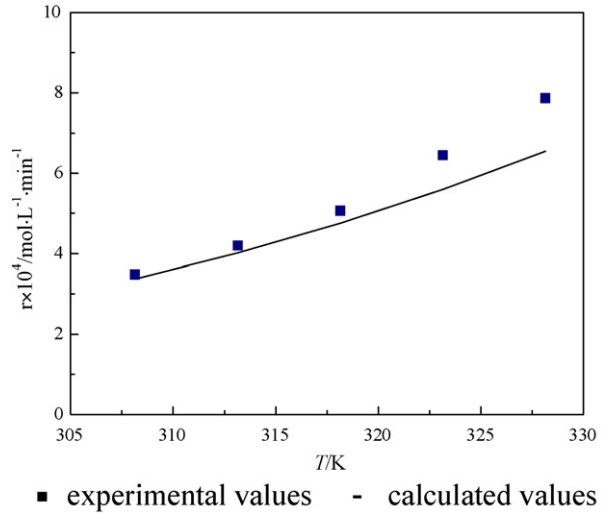

Fig. 11. Effect of temperature on the oxidation rate. Q = 140 L h^{-1}; $C_{SO_3^{2-}}$ = 0.015 mol L^{-1}; $C_{SO_4^{2-}}$ = 1.4 mol L^{-1}; pH = 5.4. (■) Experimental values; (□) calculated values.

Table 1
Values of model parameters(R, σ_L, μ_L and D_R).

Parameters	Values				
	At 308.15 K	At 313.15 K	At 318.15 K	At 323.15 K	At 328.15 K
R (J mol^{-1} K^{-1})	8.31	8.31	8.31	8.31	8.31
σ_L (mN m^{-1})	70.50	69.81	68.82	67.77	66.92
μ_L (mPa s)	0.7225	0.6559	0.5988	0.5492	0.5064
D_R (m)	0.108	0.108	0.108	0.108	0.108

Table 2
Values of model parameters(h^+, h^- and h_G) [20].

Ion species	h^+	h^-	h_G
NH_4^+	0.0290	–	–
SO_3^{2-}	–	0.0069	–
HSO_3^-	–	0.0663	–
SO_4^{2-}	–	0.0290	–
	–	–	0.028 (at 308.15 K)
	–	–	0.024 (at 313.15 K)
O_2	–	–	0.019 (at 318.15 K)
	–	–	0.015 (at 323.15 K)
	–	–	0.010 (at 328.15 K)

ues. Bubbling process in the reactor is complex and the bubble size distribution is hard to be calculated. For the sake of simplification, the bubble diameter is assumed to be the same in this paper. Thus, the calculated values could not closely correspond to the calculated values. Further investigation is needed.

5. Conclusions

Using bubbling apparatus, the kinetics of oxidation of total sulfite in ammonia-based wet FGD process was studied by varying SO_3^{2-} concentration, SO_4^{2-} concentration, pH, temperatures and air flow. The reaction was found to be −0.5 order with respect to sulfite. The oxidation rate of total sulfite is inversely proportional to the sulfate concentration. Thus, the oxidation rate of total sulfate would be inhibited to a considerably low value with too much sulfate in the solution. The experimental findings also show that the bisulfite can be oxidized easier than sulfite. Thus, keeping the pH level of the solution low is conducive to the oxidation of total sulfite. The apparent activation energy for the overall oxidation was calculated to be 28.0 kJ mol^{-1}.

A kinetic model was established on the basis of analysis of the experimental results. The developed kinetic model, including the operating parameters SO_3^{2-} concentration, SO_4^{2-} concentration, pH, temperatures and air flow, can be applied to simulate the oxidation of total sulfite. The model provided a satisfactory simulation of the experimental results for the operating conditions of SO_3^{2-} concentration, SO_4^{2-} concentration, pH and temperatures. The oxidation rate of total sulfite increases with air flow increases. However, the comparison of calculated and experimentally measured dependence of oxidation rate to air flow shows that the experimental values increase more rapidly than the calculated values. Thus, further investigation is needed.

Acknowledgment

This work was supported by the Natural Science Foundation of Jiangsu Province (BK2008421).

References

[1] H.L. Bai, P. Biswas, T.C. Keener, SO_2 removal by NH_3 gas injection: effects of temperature and moisture content, Energy Convers. Manage. 44 (1994) 1231–1236.
[2] B.S. He, X.Y. Zheng, Y. Wen, et al., Temperature impact on SO_2 removal efficiency by ammonia gas scrubbing, Energy Convers. Manage. 44 (2003) 2175–2188.
[3] Y.X. Guo, Z.Y. Liu, Z.G. Huang, et al., Reaction behavior of sulfur dioxide with ammonia, Ind. Eng. Chem. Res. 44 (2005) 9989–9995.
[4] X.L. Long, W. Li, W.D. Xiao, Novel homogeneous catalyst system for the oxidation of concentrated ammonium sulfite, J. Hazard. Mater. 129 (2006) 260–265.
[5] G.C. Mishra, R.D. Srivastava, Kinetics of oxidation of ammonium sulfite by rapid-mixing method, Chem. Eng. Sci. 30 (1975) 1387–1390.
[6] K. Neelakantan, J.K. Gehlawat, Kinetics of absorption of oxygen in aqueous solutions of ammonium sulfite, Ind. Eng. Chem. Fundam. 19 (1980) 36–39.
[7] N. Ahamd, I. Eroğlu, T. Gŭrkan, Factors affecting the kinetics of the heterogeneous oxidation of ammonium sulfite, Can. J. Chem. Eng. 65 (1987) 50–55.
[8] T. Gŭrkan, A. Nufal, I. Eroğlu, Kinetics of the heterogeneous oxidation of ammonium sulfite, Chem. Eng. Sci. 47 (1992) 3801–3808.
[9] J.H. Zhou, W. Li, W.D. Xiao, Kinetics of heterogeneous oxidation of concentrated ammonium sulfite, Chem. Eng. Sci. 55 (2000) 5637–5641.
[10] S. Bengtsson, J. Bjerle, The absorption of oxygen into sodium sulfite solution in a packed column, Chem. Eng. Sci. 30 (1975) 1429–1435.
[11] V. Linek, V. Vacek, Chemical engineering use of catalyzed sulfite oxidation kinetics for the determination of mass transfer characteristics, Chem. Eng. Sci. 36 (1981) 1747–1768.
[12] H.S. Fogler, Elements of Chemical Reaction Engineering, third ed., Prentice Hall International Series In the Physical and Chemical Engineering Science, New Jersey, 2005, pp. 177–205.
[13] M. Pisu, A. Cincotti, G. Cao, et al., Prediction of uncatalysed calcium bisulfate oxidation under operating conditions relevant to wet flue gas desulphurization plants, Chem. Eng. Res. Des. 82 (2004) 927–932.
[14] J.H. Zhou, W. Li, W.D. Xiao, The solubilities of oxygen in electrolyte solutions of ammonium salts, Oxid. Commun. 23 (2000) 172–177.
[15] E. Narita, F. Lawson, K.N. Han, Solubility of oxygen in aqueous electrolyte solutions, Hydrometallurgy 10 (1983) 21–37.
[16] L.D. Wang, Y. Zhao, Kinetics of sulfite oxidation in wet desulfurization with catalyst of organic acid, Chem. Eng. J. 136 (2008) 221–226.
[17] M. Gerbec, A. Stergarsek, R. Kocjancic, Simulation model of wet flue gas desulphurization plant, Comput. Chem. Eng. 19 (1995) 283–286.
[18] D. Thomas, S. Colle, J. Vanderschuren, Kinetics of SO_2 absorption into fairly concentrated sulphuric acid solution containing hydrogen peroxide, Chem. Eng. Sci. 42 (2003) 487–494.
[19] K. Ueyama, J. Hatanka, Salt effect on solubility of nonelectrolyte gases and liquids, Chem. Eng. Sci. 37 (1982) 790–792.
[20] B.C. Zhu, Elements of Chemical Reach Engineering, fourth ed., Chemical Industrial Press, Beijing, 2007, pp. 187–210.
[21] K. Aktia, F. Yoshida, Bubble size interfacial area and liquid-phase mass transfer coefficient, Ind. Eng. Chem., Process Des. Dev. 13 (1974) 84–91.